GRAIN REFINEMENT AND MICROSTRUCTURE EVOLUTION IN ALUMINUM A2618 ALLOY BY HIGH-PRESSURE TORSION

Intan Fadhlina Mohamed[a,c,d*], Seungwon Lee[c,d], Kaveh Edalati[c,d], Zenji Horita[c,d], Shahrum Abdullah[a,b], Mohd Zaidi Omar[a,b], Wan Fathul Hakim Wan Zamri[a,b]

[a]Faculty of Engineering and Built Environment, Universiti Kebangsaan Malaysia, 43600 UKM Bangi, Selangor, Malaysia
[b]Centre for Automotive Research, Faculty of Engineering and Built Environment, Universiti Kebangsaan Malaysia, 43600 UKM Bangi, Selangor Darul Ehsan, Malaysia
[c]Department of Materials Science and Engineering, Faculty of Engineering, Kyushu University, Fukuoka 819-0395, Japan
[d]WPI, International Institute for Carbon-Neutral Energy Research (WPI-I2CNER), Kyushu University, Fukuoka 819-0395, Japan

Abstract

This work presents a study related to the grain refinement of an aluminum A2618 alloy achieved by High-Pressure Torsion (HPT) known as a process of Severe Plastic Deformation (SPD). The HPT is conducted on disks of the alloy under an applied pressure of 6 GPa for 1 and 5 turns with a rotation speed of 1 rpm at room temperature. The HPT processing leads to microstructural refinement with an average grain size of ~250 nm at a saturation level after 5 turns. Gradual increases in hardness are observed from the beginning of straining up to a saturation level. This study thus suggests that hardening due to grain refinement is attained by the HPT processing of the A2618 alloy at room temperature.

Keywords: Severe plastic deformation, high-pressure torsion, grain refinement, Al alloy

Abstrak

Kerja ini membentangkan kajian yang berkaitan dengan penghalusan ira daripada aloi aluminium A2618 dicapai dengan kilasan tekanan tinggi (HPT) yang dikenali sebagai proses ubah bentuk plastik yang teruk (SPD). HPT dijalankan pada cakera aloi pada tekanan 6 GPa untuk 1 dan 5 pusingan dengan kelajuan putaran 1 rpm pada suhu bilik. Pemprosesan HPT membawa kepada perbaikan mikrostruktur dengan saiz ira purata ~ 250 nm pada tahap tepu selepas 5 pusingan. Peningkatan beransur-ansur dalam kekerasan diperhatikan dari awal terikan sehingga ke tahap tepu. Kajian ini sekali gus menunjukkan bahawa pengerasan kerana penghalusan ira dicapai oleh pemprosesan HPT aloi A2618 pada suhu bilik.

Kata kunci: Ubah bentuk plastik yang teruk, kilasan tekanan tinggi, penghalusan ira, Aloi Al

1.0 INTRODUCTION

The Aluminum A2618 is a heat-treatable Al-Cu-Mg-Fe-Ni alloy developed mostly for automobile and aircraft engine components industries [1,2]. When compared to other 2XXX series alloys, the A2618 alloy has good strength and stability at temperature up to 200 °C. This enhancement is attributed to the addition of Fe and

Ni contributing to the microstructure stability of the alloy under thermal condition [3].

The strength of A2618 can be attained from a conventional aging process. However, a much higher strength may be possible by further refining grain size through the Hall-Petch relation [4,5]. Application of severe plastic deformation (SPD) process leads to grain refinement regardless of sample states including supersaturation of solute atoms [6]. Several SPD processes are available, such as high-pressure torsion (HPT), equal-channel angular pressing (ECAP), accumulative roll bonding (ARB) and etc., which allow grain refinement of alloys to the submicrometer or nanometer levels [7,8].

The principle of the HPT process has been introduced in 1935 by Bridgman [9]. With the HPT process, the material is deformed between two anvils by rotating them with respect to each other under a high hydrostatic pressure. It is gaining much interest because the process leads to generation of a high density of dislocations that rearrange into subgrains and finally form ultrafine grains with high-angle boundaries [9-12]. It was reported that additional straining by the HPT process has further reduced the grain size in comparison with the ECAP process [9,11].

Although the HPT process has been applied to many Al alloys, there is no report that it has applied to a commercial A2618 alloy. The objective of this research is thus to investigate mechanical properties and microstructure changes in the A2618 alloy after HPT processing at room temperature.

2.0 EXPERIMENTAL PROCEDURE

The material used in this study was a commercial A2618 alloy with an initial grain size of 40 μm in average. The material was received in a form of rod with 20mm diameter. Disk of 10mm diameter and 1mm thickness was then cut from the rod by a wire-cutting electrical discharge machine (EDM). The disks were subjected to solution treatment at 540 °C for 12 hr in an air atmosphere and then immediately quenched in ice water.

Each sample with 1mm thickness was processed by HPT at room temperature (RT) under an applied pressure of 6 GPa for two different turns (N) as 1 and 5. The rotation speed was set to 1 rpm. The thicknesses after 1 and 5 turns were reduced to 0.83 mm and 0.80 mm respectively by the HPT-processing. These thicknesses were used later for the calculation of the equivalent strain as in an earlier report [13].

The disks were polished to a mirror-like surface and the Vickers microhardness was measured by application of 100 g for 15 s using a Mitutoyo HM-102 tester. The measurements were made at equal distances from the disk center to the edge along 8 different radial directions as illustrated in Fig. 1.

The HPT-processed samples were grounded to a thickness of 0.4 mm, punched to small disks with 3mm diameters as shown in Fig. 1. They were further ground to a thickness of 0.12 mm. The samples were thinned to perforation for transmission electron microscopy (TEM) using a twin-jet electro-polisher in a solution of 25% HNO_3 and 75% C_2H_5OH at a temperature of 263 K under an applied voltage of 15 V. Microstructures were observed using a conventional transmission mode with parallel beam using Hitachi H-8100 TEM at an accelerating voltage of 200 kV. Selected-area electron diffraction (SAED) patterns were taken around regions of 6.3 μm in diameter.
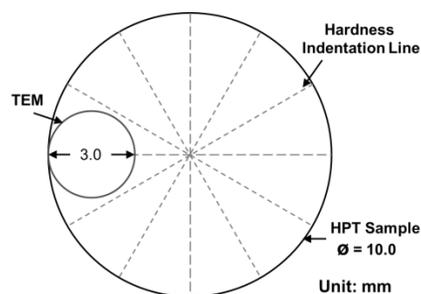

Figure 1 Schematic illustration of HPT disk and locations for hardness measurements and TEM disk

3.0 RESULTS

3.1 Hardness

Figure 2(a) plots microhardness as a function of distance from the disk center after 1 and 5 turns. The hardness after the HPT processing increased drastically above the solution-treated sample indicated by a dotted line. The hardness increases with increasing distance from the disk center and saturates at a constant level when approaching the edge of the disk. The increase is more prominent after 5 turns than 1 turns as shown in Fig. 2(a). The saturation of the hardness level appears in the disk for N = 5. However, after 1 turn, the increase in hardness was closer to the saturation level approaching the edge of the sample.
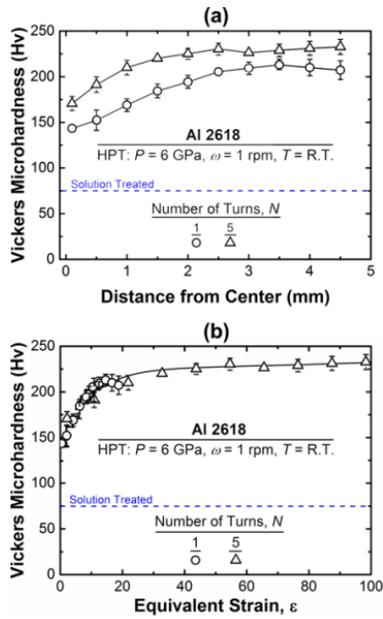
Figure 2 Vickers microhardness vs *(a) distance from disk centre and (b) equivalent strain*

The hardness values in Fig. 2(a) are re-plotted as a function of equivalent strain in Fig. 2(b) as in earlier papers [13-22]. It is well known that the equivalent Von Mises strain ε imposed on the sample processed by HPT is given by Equation 1 [7,18]:

$$\varepsilon = \frac{2\pi r N}{\sqrt{3}t} \qquad (1)$$

where r is the distance from the disk center, N is number of turns and t is the thickness of disk. As in Fig. 2(b), the hardness variation is well represented by a unique function of the equivalent strain. The hardness increases rapidly at the beginning of straining, levels off at the equivalent strain of ~20 before it enters a steady state level where the hardness remains unchanged at a constant level of Hv ≈ 230 HV with further straining. In earlier studies, a similar behavior of the hardness with respect to straining was reported in many pure metals and alloys [14,16,19,21,23-28].

3.2 Microstructure

Figure 3 shows a series of bright-field images (left) and dark-field images (centre) and the corresponding SAED patterns (right) after HPT processing for (a) $N = 1$ ($\varepsilon \approx 17$) and (b) $N = 5$ ($\varepsilon \approx 70$). The arrows in the SAED patterns indicate diffracted beams used for taking the dark-field images. The grain boundaries appeared curved and ill-defined, which is a typical feature as often observed in SPD-processed materials. For $N = 1$ corresponding to the stage before entering the saturation level, a higher density of dislocations is observed within the grain as seen in the bright-field and dark-field images in Fig. 3(a). The SAED pattern

displays less spots around rings, indicating low misorientation angles between the grains. This observation thus corresponds to the intermediate stage where the formation of subgrains occurs at medium straining before entering saturation state. At larger strains as after $N = 5$, the hardness increases to the saturated level and the grain evolves to a more fraction of smaller sizes. The microstructural change occurs by conversion of low-angle to high-angle boundaries while the fine grains being retained [28]. This is confirmed by the appearance of extra spots in the SAED pattern to be distributed in a ring form with increasing straining. TEM observation in Fig. 3 thus confirms that grain refinement is achieved to grain sizes of ~250 ± 100 nm and ~250 ± 40 nm after the HPT processing through $N = 1$ and $N = 5$, respectively.

4.0 DISCUSSION

Based on the hardness variation in Fig. 2 and the microstructure evolutions in Fig. 3, the grain refinement in A2618 may be achieved in the same way as the previous study [29]. At the beginning of the straining, many dislocations were generated by normal deformation mode and coalescence to form subgrain boundaries. The dislocations accumulated with further straining and increase the density within the subgrains. Finally, the formation of smaller grain size is obtained when the width of subgrain becomes better defined with increasing misorientation angle [30] as shown by Fig. 3(a) and (b).
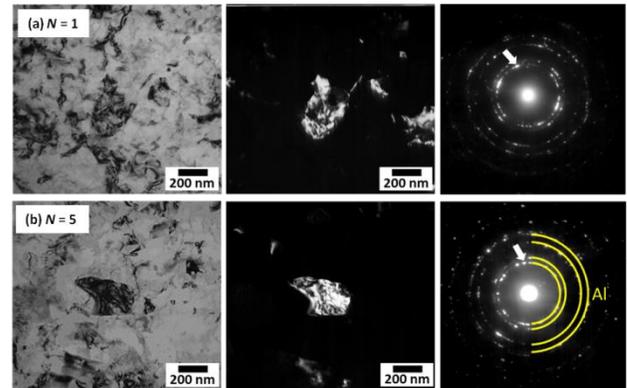

Figure 3 TEM micrographs and SAED patterns of A2618 after HPT processing at *(a) initial stage before entering saturation (N = 1) and (b) saturated stage (N = 5). Arrows in SAED patterns indicate diffracted beams for dark-field images*

5.0 CONCLUSIONS

The brief conclusions of this work are presented below:
(1) The grain size was refined to ~250 ± 40 nm and microhardness was significantly increased through application of HPT processing.

(2) The hardness values after 1 and 5 turns fell well on a single curve when they are plotted against the equivalent strain.

(3) The hardness increases with straining by HPT and saturates to a constant level at 230 HV after the HPT processing for 5 turns.

Acknowledgements

References

[1]   ASM International Handbook Committee, Metals Handbook. 1979. *Properties and Selections: Nonferrous Alloys and Pure Metals*, 10th Ed. ASM International: The Materials Information Company P. 81-2.

[2]   C. Williams James, A. Starke Jr Edgar. 2003. Progress in Structural Materials for Aerospace Systems, *Acta Materialia*. 51(19): 5775–5799.

[3]   Y. Kun, L. Wenxian, L. Songrui, Z. Jun. 2004. Mechanical Properties and Microstructure of Aluminum Alloy 2618 with Al3(Sc, Zr) Phases, *Materials Science and Engineering*. A 368: 88–93.

[4]   E.O. Hall. 1951. The Deformation and Ageing of Mild Steel: 111 Discussion of Results, *Proceeding of Physical Society*. B 64: 747.

[5]   N.J. Petch. 1953. The Cleavage Strength of Polycristals, *The Journal of Iron and Steel Institute*. 174: 25.

[6]   Z. Horita, T. Fujunami, M. Nemoto, T.G. Langdon. 2001. Improvement of Mechanical Properties for Al Alloys Using Equal-Channel Angular Pressing, *Journal of Materials Processing Technology*. 117: 288-292.

[7]   R.Z. Valiev, R.K. Islamgaliev, I.V. Alexandrov. 2000. Bulk Nanostructured Materials from Severe Plastic Deformation, *Progress in Materials Science*. 45: 103-189.

[8]   R.Z. Valiev, Y. Estrin, Z. Horita, T.G. Langdon, M.J. Zehetbauer, Y.T. Zhu. 2006. Producing Bulk Ultrafine-grained Materials by Severe Plastic Deformation, *JOM* 58(4): 33-39.

[9]   P.W. Bridgman. 1935. Effect of High Shear Stress Combined with High Hydrostatic Pressure, *Physical Review*. 48: 825-847.

[10] V.V. Stolyarov, Y.T. Zhu, T.C. Lowe, R.K. Islamgaliev, R.Z. Valiev. 1999. A Two Step SPD processing of ultrafine-grained titanium, *Nanostructured Materials*. 11: 947-954.

[11] Y. Iwahashi, Z. Horita, M. Nemoto, T.G. Langdon. 1998. Factors Influencing the Equilibrium Grain Size in Equal-Channel Angular Pressing: Role of Mg Additions to Aluminum, *Metallurgical and Materials Transactions A* 29A: 2503-2510.

[12] Z. Horita, D.J. Smith, M. Furukawa, M. Nemoto, R.Z. Valiev, T.G. Langdon.1996. An Investigation of Grain Boundaries in Submicrometer-grained Al-Mg Solid Solution Alloys using High-Resolution Electron Microscopy, *Journal of Materials Research* 11: 1880-1890.

[13] A.P. Zhilyaev, S. Lee, G.V. Nurislammova, R.Z. Valiev, T.G. Langdon. 2001. Deformation Heating and Its Effect on Grain Size Evolution during Equal Channel Angular Extrusion, *Scripta Materialia* 44: 2753-2758.

[14] A. Vorhauer, R. Pippan. 2004. On the Homogeneity of Deformation by High Pressure Torsion, *Scripta Materialia* 51: 921-925.

[15] K. Edalati, T. Fujioka, Z. Horita. 2008. Microstructure and Mechanical Properties of Pure Cu Processed By High-Pressure Torsion, *Materials Science and Engineering A* 497 168-173.

[16] K. Edalati, T. Fujioka, Z. Horita. 2009. Evolution of Mechanical Properties and Microstructures with Equivalent Strain in Pure Fe Processed by High Pressure Torsion, *Materials Transactions* 50: 44-50.

[17] S. Lee, K. Edalati, Z. Horita. 2010. Microstructures and Mechanical Properties of Pure V and Mo Processed by High-pressure Torsion, *Materials Transactions* 51:1072-1079.

[18] I.F. Mohamed, S. Lee, Z. Horita. 2013. Strengthening of Al 6061 Alloy by High-Pressure Torsion Through Grain Refinement and Aging, *Materials Science Forum* 765: 408-412.

[19] I.F. Mohamed, Y. Yonenaga, S. Lee, K. Edalati, Z. Horita. 2015. Age Hardening and Thermal Stability of Al–Cu Alloy Processed by High-Pressure Torsion, *Materials Science and Engineering. A* 627: 111-118.

[20] S. Lee, K. Tazoe, I.F. Mohamed, Z. Horita. 2015. Strengthening of AA7075 Alloy by Processing with High-pressure Sliding (HPS) and Subsequent Aging, *Materials Science and Engineering. A* 628: 56-61.

[21] I.F. Mohamed, S. Lee, K. Edalati, Z. Horita, S. Hirosawa, K. Matsuda, D. Terada. 2015. Aging Behavior of Al 6061 Alloy Processed by High-Pressure Torsion and Subsequent Aging, Metallurgical and *Materials Transactions. A* 46(6): 2664-2673.

[22] J.M. Cubero-Sesin, M. Arita, Z. Horita. 2015. High Strength and Electrical Conductivity of Al-Fe Alloys Produced by Synergistic Combination of High-Pressure Torsion and Aging, *Advanced Engineering Materials*. 17: 1792-1803.

[23] K. Edalati, Z. Horita. 2013. Application of High-Pressure Torsion for Consolidation of Ceramic Powders, *Scripta Materialia*. 63: 174-177.

[24] A.P. Zhilyaev, T.G. Langdon. 2008. Using high-pressure torsion for metal processing: Fundamentals and applications, *Progress in Materials Science*. 53: 893-979.

[25] K. Edalati, E. Matsubara, Z. Horita. 2009. Processing pure Ti by high-pressure torsion in wide ranges of pressures and strain, Metallurgical and *Materials Transaction. A*(40A): 2009-2079.

[26] Y. Harai, K. Edalati, Z. Horita, T.G. Langdon. 2009. Using ring samples to evaluate the processing characteristics in high-pressure torsion, *Acta Materialia*. 57: 1147-1153.

[27] J.M. Cubero-Sesin, Z. Horita. 2015. Age Hardening in Ultrafine-Grained Al-2 pct Fe Alloy Processed by High-Pressure Torsio, Metallurgical and *Materials Transaction. A*(46)A: 2614-2624.

[28] S. Lee, Z. Horita, S. Hirosawa, K. Matsuda. 2012. Age-hardening of An Al-Li-Cu-Mg Alloy (2091) Processed by High-Pressure Torsion, *Materials Science and Engineering. A* 546: 82-89.

[29] B.Q. Han, E.J. Lavernia, F.A. Mohamed. 2003. Dislocation Structure and Deformation in Iron Processed by Equal-Channel-Angular Pressing, *Metallurgical and Materials Transactions. A*(35A): 1343-1350.

[30] Y. Ito, Y. Harai, T. Fujioka, K. Edalati, Z. Horita. 2008. *Materials Science Forum*. 584-586: 191-196.